Journal of Aerosol Science 42 (2011) 621–630

Contents lists available at ScienceDirect

Journal of Aerosol Science

journal homepage: www.elsevier.com/locate/jaerosci

Electrohydrodynamic pulsed-inkjet characteristics of various inks containing aluminum particles

D.K. Kang [a], M.W. Lee [a], H.Y. Kim [a], S.C. James [b], S.S. Yoon [a,*]

[a] School of Mechanical Engineering, Korea University, Anamdong, Seongbukgu, 5-Ga 1-Bungi, 136-701 Seoul, Republic of Korea
[b] Thermal/Fluid Science & Engineering, Sandia National Laboratories, P.O. Box 969, Livermore, CA 94551, USA

ARTICLE INFO

Article history:
Received 31 January 2011
Received in revised form
20 June 2011
Accepted 20 June 2011
Available online 24 June 2011

Keywords::
EHD (Electrohydrodynamics)
Inkjet printing
Aluminum
Suspension

ABSTRACT

As nano-sized silver particles are prohibitively expensive, lower cost materials (e.g., micro-sized aluminum) are sought for the manufacture of conducting electrodes. Inks containing various aluminum weight percentages are dot-printed onto a stainless-steel substrate with an electrohydrodynamic (EHD) inkjet, which is superior to thermal and piezoelectric inkjets for inks containing larger particles because it ejects drops smaller than the nozzle diameter. Various ink solvents (ethanol, octanol, and diethylene glycol) are formulated with aluminum particles from 1 to 10 wt%. EHD inkjet characteristics such as drop-separation distance, drop size, drop-to-substrate impact velocity, and required voltage are reported. The ink's thermo-fluid properties are the primary factors controlling drop characteristics and printing quality.

1. Introduction

Inkjet technology has broad application to everything from printed electronics, to drug discovery, to micromechanical devices (Cheng et al., 2005; Jaworek & Sobczyk, 2008; Miao & Xiao, 2002). Its ability to pattern various materials, its compatibility with large-area substrates, its highly accurate targeting, its relatively simple application (as compared to photolithography), and its non-vacuum and non-contact printing approach makes it attractive and suitable to more than just the various applications mentioned above.

Other printing technologies generate drops through ink boiling (i.e., bubble jet) or by piezoelectric nozzle deformation (squeezing) (Chen et al., 1997, 1999; Xu et al., 2005), but yield in flexible drop-size control, which is achieved only by scaling the nozzle dimension because drop size is comparable to nozzle size. This drop-to-nozzle scaling is inefficient because each nozzle must be manufactured at a scale commensurate with the required drop size.

EHD inkjet printing has the advantage that drop size can be manipulated with the applied voltage frequency (Lee et al., 2008). The advantage of using a single, relatively large nozzle to produce a variety of drop sizes is obvious (Kim et al., 2008), not only because costly micro-scale nozzle manufacture can be avoided, but because the nozzle can be sufficiently large to allow use of lower cost larger particles. Moreover, larger nozzles are much less likely to clog. Finally, the "coffee-ring" effect (Park & Moon, 2006; Singh et al., 2010), where colloidal metal particles migrate towards the periphery of the evaporating drop and leave residues, is decreased when using larger particles. This use of larger particles is a significant advantage for designing electrodes because irregular dispersions of nano-scaled small particles showing the coffee-ring effect yield poor conductors.

* Corresponding author.
E-mail address: skyoon@korea.ac.kr (S.S. Yoon).

0021-8502/$ - see front matter © 2011 Elsevier Ltd. All rights reserved.
doi:10.1016/j.jaerosci.2011.06.009

Jayasinghe et al. (2002) printed 30–400-μm dots (or "relics," which are dried inkjet drops) using an EHD technique. Their solvent was ethanol containing 0.5-μm alumina ceramic particles between 20 and 60 wt%. Samarasinghe et al. (2006) also used an EHD inkjet to produce 75-μm relics using an ethanol solvent containing 15-nm gold particles at 10 wt%. Their drop-size distribution was Gaussian with a 30-μm mean while the inner diameter of their nozzle was 200 μm. Because of the relatively low weight percentage and the Benard–Marangoni effect (Wasan et al., 2001), their printed line was discontinuous. Using an EHD inkjet with a 500-nm MEMS-manufactured nozzle, Park et al. (2007) produced 490-nm relics. Their solvent was a blend of 3,4-ethylenedioxythiophene and styrenesulphonate containing no solid particles. Paine et al. (2007) printed 1.4 μm-size relics on a surface with a targeting accuracy of a few microns. Mishra et al. (2010) demonstrated high-speed (1 kHz) printing capabilities yielding 3–5-μm relics using a phosphate buffer solution and 1–2-μm relics for a photocurable polyurethane polymer ink. This was a significant result because it demonstrated that EHD printing is capable of high-speed (i.e., 1000 drop/s) and high-resolution (1–2 μm) printing. They also showed how the printing deposition rate could be controlled by varying the voltage pulse width and frequency.

In case of sufficient supply of voltage, the EHD inkjet mode changes, generally from the discrete pulsing mode to the continuous cone-jet mode. Korkut et al. (2008) printed arrays of colloidal suspensions on hydrophobic surfaces with nozzles of 340- and 510-μm inner diameters using the continuous cone-jet mode. Their solvent was polyethylene oxide containing polystyrene particles with mean diameter and concentrations of 3.1 μm and 6–15 wt%, respectively. Eight micrometer relics were observed using their solvent without particles. Paine (2009) also confirmed the mode change from the pulsed mode to the cone-jet mode when increasing the voltage level.

One apparent hole in the literature is that the fluid-dynamic characteristics of EHD inkjets (e.g., drop shape and topology, nozzle-to-drop separation distance, drop size, and drop-to-substrate impact velocity) have not been well addressed. These characteristics depend upon the thermo-fluid properties of the inks, primarily viscosity and surface tension, suggesting that the choice of ink can influence the ultimate quality of relics. For example, if an ink's viscosity is too low, a drop readily separates from the nozzle, but undesirable satellites drops may form and relic size can increase due to increased spreading of a drop upon impact. On the other hand, if viscosity is too high, satellite formation is suppressed, but the ink may not separate from the nozzle (drop generation failure). Thermo-fluid properties of the inks should be selected for the specific application requirements. Drop-generation behavior subject to operating conditions, such as applied voltage and frequency, also needs to be scrutinized. This paper studies the drop-generation behavior and printing quality of various EHD inks. Moreover, we report the drop-generation behavior and printing quality of the EHD inkjet under various operating conditions (voltage and frequency).

2. Experimental setup

Fig. 1 shows the inks studied; three alcohol-based solvents (Duksan Chemical), ethanol, octanol, and diethylene glycol (DEG), contain 5–10-μm Al particles (Yee Young Cerachem, LTD). To promote particle dispersion, zirconia beads (i.e., white marbles at container bottoms in Fig. 1) are added to break up any aggregated particles when the container is shaken (so called, ball-milling). The octyl alcohol-based suspension had the most sedimentation (or poorest dispersion stability) after 8 h. There are two simple ways to increase dispersion stability; increase particle Brownian motion by increasing the solvent's acidity such that a proton-exchange mechanism opposes sedimentation (Hughes et al., 1999), or increase the surface potential by adding sodium so that particles inter-repulsion is increased.

Given that the buoyant force depends on fluid density, added salt can help keep particles afloat. That is, increased density due to salinity helps hold particles in suspension longer (decreases settling speed); hence, printing quality is improved because particle concentrations are more uniform. However, all additives leave residues, some of which may hinder the electrical performance of the printed device. A total of 0.4 g of sodium alginate was added to all bottles in Fig. 1 (0.4 g/10.4 g = 3.85 wt%). Despite adding sodium, sedimentation was still evident (see Fig. 1) because Al particles are simply too large for these techniques to work.

Fig. 2 is a schematic of the experimental setup for the EHD printing system. Al ink in ethanol, octanol, or DEG is supplied to the stainless-steel nozzle (EFD, 18 gage, inner and outer diameters of 0.84 and 1.27 mm, respectively) by a syringe pump (KDS 100). A multi-function synthesizer (NF Corporation, WF 1973) generates a rectangular step-function signal, which is sent to the HV-amplifier (TREK 10/40A) for thousand-fold amplification. The width of the rectangular signal (duty ratio) was held constant at 2 ms, which is 0.2% of the time when $f=1$ Hz and 2% of the time when $f=10$ Hz. Given the 2-ms duty ratio, frequencies in excess of 500 Hz are not possible here. Although higher frequencies could be imposed with a commensurately shorter duty ratio, it would preclude a consistent comparison of drop properties. In this work, no baseline (or bias) low-voltage was applied, although this could facilitate preloading of the liquid meniscus for easier drop ejection at each voltage peak.

A high-speed camera (Vision Research, Inc., Phantom 7.3) with zoom lens (1.56 μm/pixel) and Halogen lamp (250 W) captured magnified images of ejected ink drops. Snapshots are taken at 200-μs intervals. The motorized stage holding the substrate (Future Science, FS-XY-0.1-100) can maneuver up to a maximum distance of 100 mm in 0.1-μm increments. The distance between the nozzle tip and the substrate is fixed at $H=5$ mm (Fig. 1). Any shorter distance could cause an electrical arc (so called "corona discharge") between the nozzle and substrate for voltages in excess of 6 kV. The distance could be shorter (i.e., less than $H<1$ mm) if the supplied voltage was decreased. Chen et al. (2006) and Byun et al. (2008)

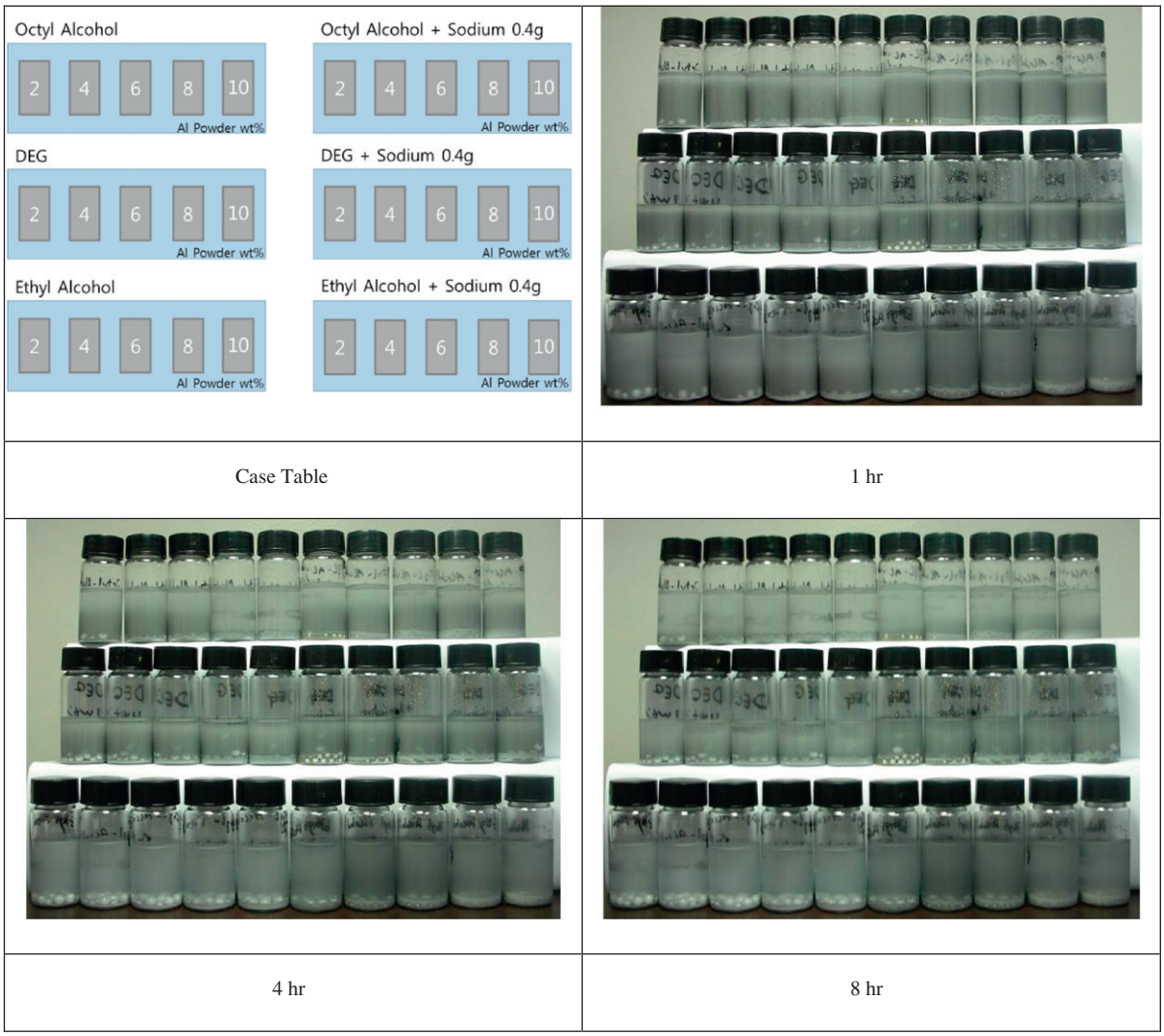

Fig. 1. Sedimentation tests for various inks.

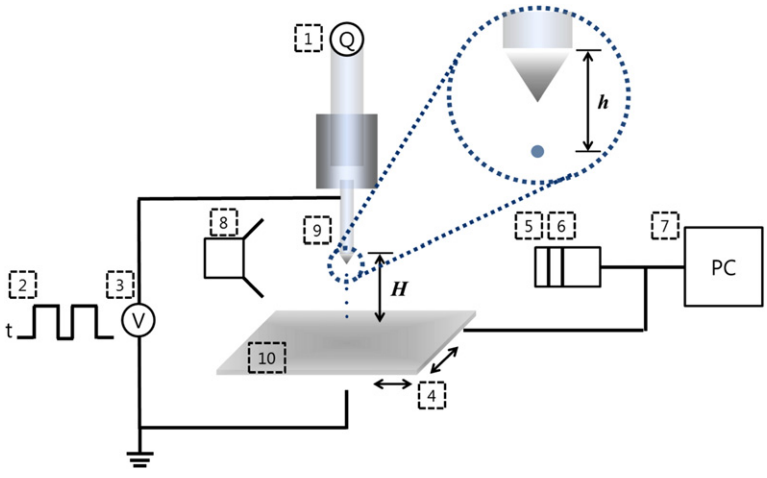

Fig. 2. Schematics (1. syringe pump, 2. multi-function synthesizer, 3. AC-amplifier, 4. stage, 5. zoom lens, 6. high-speed camera, 7. control PC, 8. light, 9. nozzle, and 10. substrate).

used $H=0.14$ and 0.2 mm when the supplied voltage was 1.2 and 0.2 kV, respectively. For optimum performance, the supplied voltage must be adjusted appropriately for each ink's thermo-electrical properties.

3. Results and discussion

Fig. 3 shows the pulsed drop formation for ethanol, octanol, and DEG inks without particles for a voltage frequency of 1 Hz. For inks with the lowest and highest viscosities, μ, and surface tensions, σ (ethanol and DEG, respectively), drops are formed. However, for octanol with $\mu_{oct}=8.4$ mPa s and $\sigma_{oct}=27.6$ mN/m, a continuous stream issues. This demonstrates potential drop-generation failure when frequency is inappropriate for μ and σ. When μ and σ are low (as is the case for the ethanol ink), drops readily gets detached from the nozzle as the fluid is more responsive to the applied voltage. Unfortunately, high sensitivity could also cause the fluid to be responsive to multiple waves from a single voltage pulse, which might lead to satellite drop formation. Also, fluids with low μ and σ spread more easily upon impact; this could lead to excessive relic size due to the increased spreading. On the other hand, when μ and σ are high, drops are more difficult to detach from the nozzle because high μ and σ tend to damp the EHD pulse. Fig. 3 lists the drop sizes of ethanol and DEG at 1 Hz; the DEG drop is larger because of its higher viscosity. It is also possible that the electrostatic force is too weak, due to extremely low conductivity of octanol, to detach a drop from the emanating liquid.

Several theoretical models are available with which to compare our experimental results. Marginean et al. (2006a, 2006b) applied Rayleigh's model to an electrified liquid meniscus at the end of a glass capillary tube; they assumed that the frequency of the lowest excitation mode for a negligible charge is

$$f \approx \left(\frac{2}{\pi^2}\frac{\sigma}{\rho r_a^3}\right)^{1/2}, \tag{1}$$

where r_a is the anchoring (capillary tube) radius.

Chen et al. (2006) also provide a natural frequency estimate for an EHD pulsed inkjet. Under the assumptions that the jet diameter is much smaller than the nozzle diameter and that the fluid is highly conductive (i.e., $>10^{-5}$ S/m), the

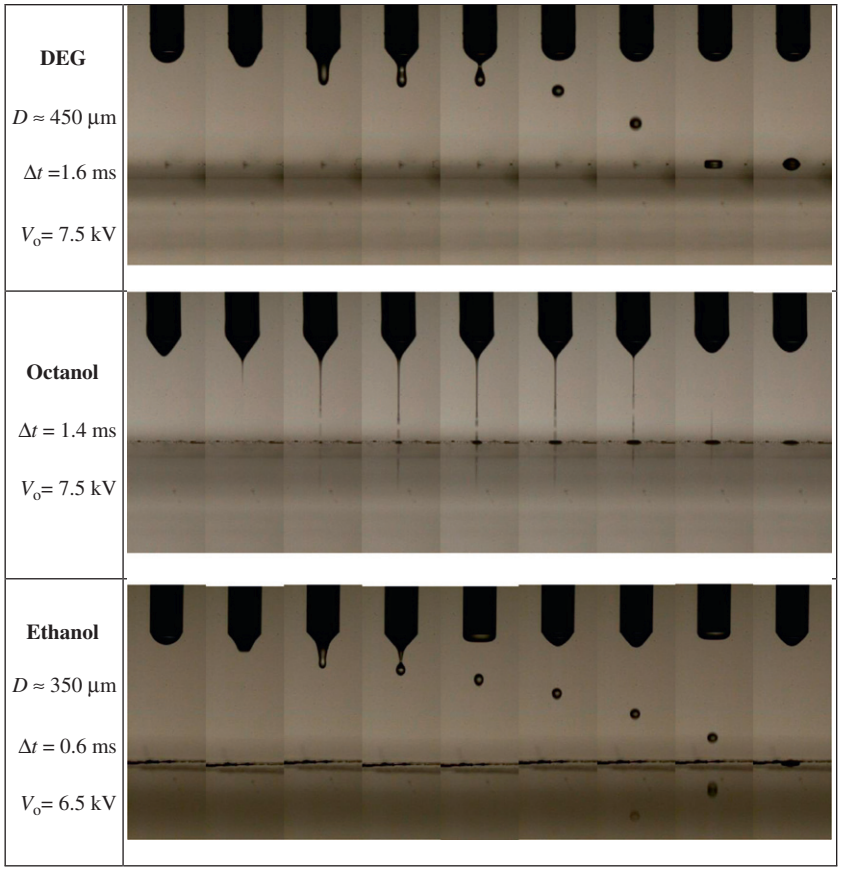

Fig. 3. Drop formation at $f=1$ Hz. Here, Δt refers to the time interval over which these snapshots were taken.

following model is suggested:

$$f \approx \frac{KE^2}{\kappa\mu L_n}\left(\frac{\rho d_n^5}{\sigma}\right)^{1/2}, \tag{2}$$

where K, κ, μ, σ, and ρ are the electrical conductivity, dielectric constant, viscosity, surface tension, and density of the working fluid, respectively, L_n and d_n are the nozzle length and diameter and E is the electric field approximated by Marginean et al. (2006a, 2006b) as $E=4V_o/[d_n \ln(8H/d_n)]$. Both Marginean et al. (2006a, 2006b) and Chen et al. (2006) fixed the voltage and then identified the frequency that yielded a stable pulsed jet. For the research presented here, it was just the opposite: the frequency was fixed (because a fixed drop deposition rate is desired) and the voltage selected to yield a stable pulsed jet. Neither Marginean et al. (2006a) nor (2006b) printed their pulsed drops onto a substrate and thus it is not known whether their high frequency (i.e., a few kHz) output would actually work for consistent printing. Mishra et al. (2010) demonstrated high-speed printing with 1 kHz frequency by printing the letter "I" with 2200 drops over 70 s, which suggests that their EHD system did not achieve 1000 drops per sec despite their voltage frequency of 1 kHz (a drop-generation rate of 31 Hz). This demonstrates a common problem associated with high frequency (i.e., a few kHz) voltages not being reflected in the rate of drop ejection. Because liquid is imperfectly conducting and has non-zero viscosity, the applied voltage cannot be perfectly reflected in the drop ejection rate. Stachewicz et al. (2009) had difficulty producing drops for frequencies exceeding 500 Hz, which is consistent with our argument in conjunction with Fig. 2.

Choi et al. (2008) also suggested modified form of Eq. (2) after assuming that an instability occurs when the surface tension force across the nozzle (σd_n) is commensurate with the electric force acting on the jet (i.e., $\varepsilon_0 E^2 d_j^2$ where d_j is the jet diameter)

$$f \approx \left(\frac{\varepsilon_0^3}{\rho^2\sigma}\right)^{1/4}\frac{E^{3/2}}{d_n^{3/4}}, \tag{3}$$

where ε_0 is the permittivity of free space. The three preceding equations were used to compute theoretical frequencies for our solvents (i.e., ethanol, octanol, and DEG) in Table 1. The theoretical frequencies exceed the frequencies applied in our experiments. Differences are attributed to the fact that the liquids are imperfect conductors, they have non-zero μ, and that the drop size is comparable to the nozzle diameter (see assumptions of Chen et al. (2006) for Eq. (2)), all of which violate the assumptions used to develop the aforementioned equations. Furthermore, it is possible that there may be a significant charge leakage in an experiment, and these effects are not considered in the theoretical formulations. Finally, the three theoretical equations for frequency do not even agree well with one another suggesting that significant variability should be expected.

The distance between the nozzle tip to the substrate (i.e., H) is an important parameter. Shorter distances or H between the nozzle and substrate allow for decreased travel time before impact. High-speed printing thus requires that the drop separate from the nozzle quickly, over a short distance, h (see Fig. 4). Smaller h allows smaller H, which increases targeting reliability (assuming no electric discharge between the nozzle and substrate). This short distance is desirable for high-speed printing because the substrate can only be moved after drop impact has occurred. Fig. 4 shows how the nozzle-to-drop separation distance varies with the applied voltage frequency; the higher the frequency, the smaller the h. This pattern is true for both ethanol and DEG solvents. The distance, h, is shorter for ethanol than DEG because ethanol has a lower viscosity (see Table 1), which facilitates drop detachment, while a more viscous fluid (i.e., DEG) has a propensity to

Table 1
Properties of the working fluids at 20 °C.

	Ethyl alcohol (C_2H_6O)	Octyl alcohol ($C_8H_{18}O$)	Diethylene glycol ($C_4H_{10}O_3$)
MW (g/mol)	46.07	130.23	106.12
ρ (kg/m^3)	789	824	1118
σ (mN/m)	22.1	27.6	44.8
μ (mPa s)	1.2	8.4	38.5
K (μS/cm)	0.7	$K<0.01$	0.24
ε	24.3 at 25 °C	3.4 at 17.8 °C	6.66 at 30 °C
D (μm)	$174<D<406$	N/A	$200<D<452$
h (mm)	$0.75<h<1.5$	N/A	$1.05<h<1.65$
u (m/s)	$1.16<u<2.03$	N/A	$1.49<u<2.40$
$We=\rho u^2 D/\sigma$	$40<We<124$	N/A	$47<We<120$
$Re=\rho Du/\mu$	$310<Re<233$	N/A	$19<Re<14$
$Oh=(We)^{0.5}/Re$	$0.02<Oh<0.05$	N/A	$0.35<Oh<0.79$
$Ca=We/Re$	$0.13<Ca<0.53$	N/A	$2.38<Ca<8.64$
$u_{char}=\sigma/\mu$ (m/s)	18.4	3.3	1.2
$l_{char,\mu}=\mu^2/\rho\sigma$ (μm)	0.082	3.1	29.6
$l_{char,\sigma}=(\sigma/\rho g)^{1/2}$ (μm)	1689	1847	2021
(1) Marginean et al. (2006a, 2006b)	277	303	331
(2) Chen et al. (2006)	$1.19\times10^8<f<1.46\times10^8$	N.A. (K is not available)	$4.30\times10^7<f<4.42\times10^7$
(3) Choi et al. (2008)	$2178<f<2539$	2498	$9316<f<9515$

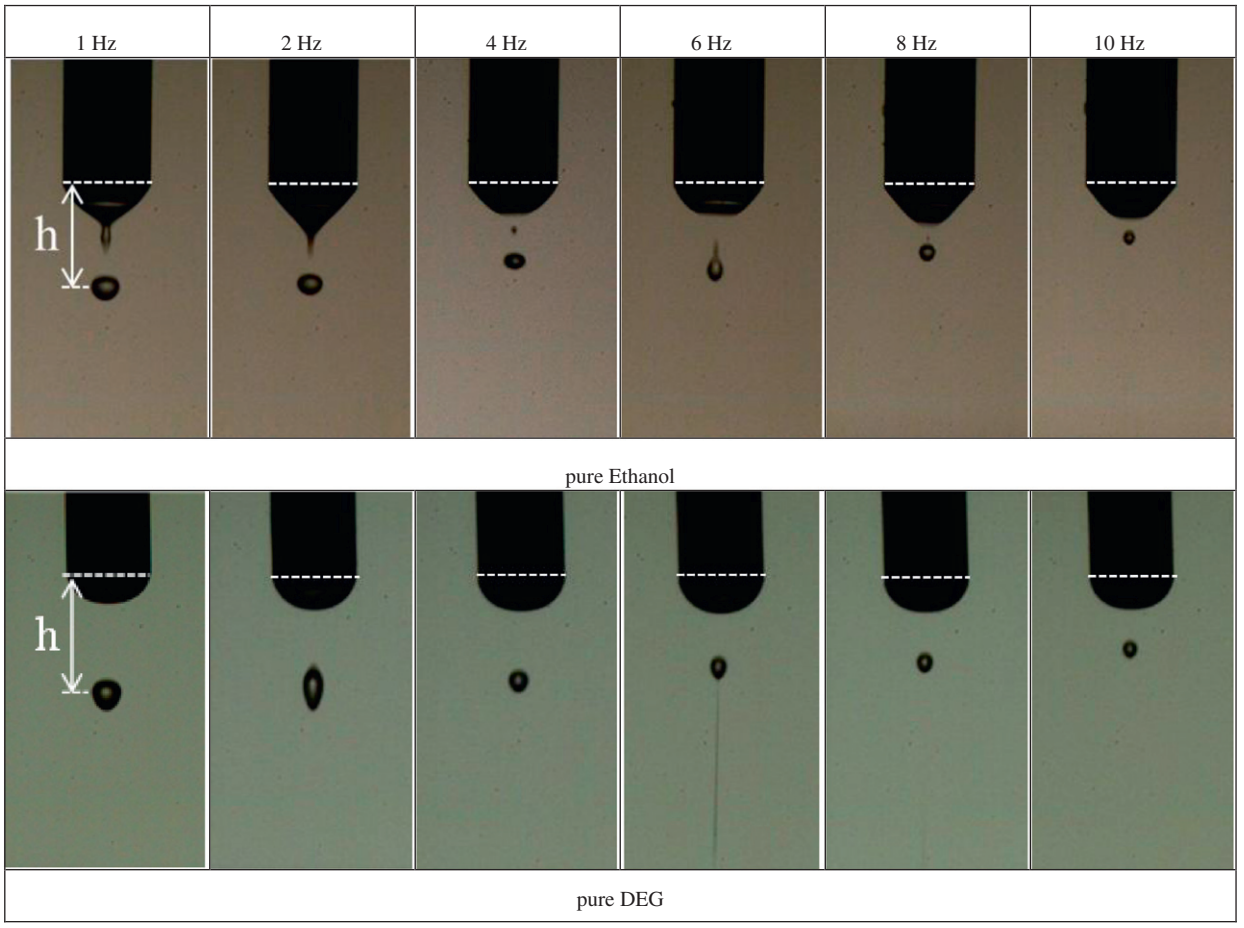

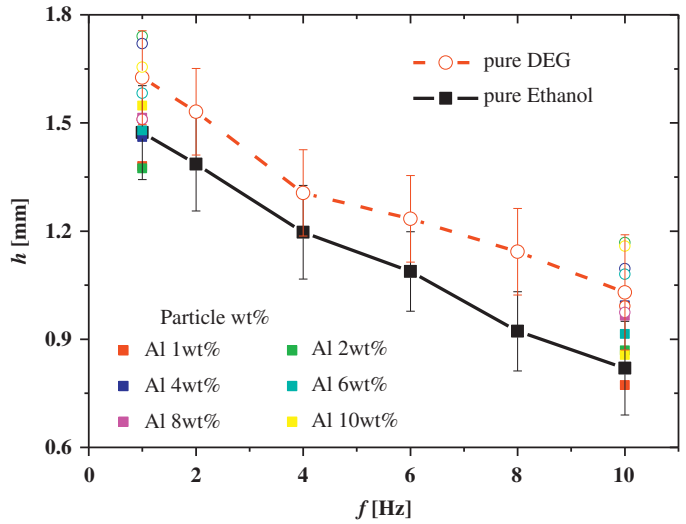

Fig. 4. Distance between the nozzle tip and drop separation, h, as a function voltage frequency, f.

elongate the detachment process as in fiber or string generation, similar to viscoelastic electrospinning (Yarin et al., 2001). Fig. 4 also shows that h is fairly independent of Al concentrations between 1 and 10 wt% suggesting that the thermo-fluid properties control drop-generation behavior, rather than the weight fraction of particles. From Fig. 4, it is interesting to note that the pure DEG drop at 6 Hz undergoes the Rayleigh explosion (or jet). This "jetting" occurs when the droplet charge exceeds the Rayleigh limits (Rayleigh, 1882), $Q=8\pi^2\varepsilon_0\sigma D^3$, that is, when the fissility $X=Q^2/(64\pi^2\varepsilon_0\sigma a^3)$ is greater than unity, where D and a are the drop diameter and radius, respectively. Duft et al. (2003) experimentally showed the

production of this Rayleigh jets. This phenomenon may degrade printing quality as the pulsed drop can eject numerous nanoscale charged satellite drops (although these satellite drops could evaporate before deposition).

Fig. 5 compares the size of the incipient drop (not the relic) of ethanol and DEG for voltage frequencies from 1 to 10 Hz; both ethanol and DEG drop sizes decrease with frequency. The incipient drop size of the DEG-based ink is greater than that for the ethanol-based ink because DEG's viscosity and surface tension are higher than ethanol's. In particular, it is the ratio of viscosity length-scale of DEG-to-ethanol (i.e., $l_{\mu,\mathrm{DEG}}/l_{\mu,\mathrm{eth}}=360$) explains the disparity because the ratio of surface tension length scale of DEG-to-ethanol is only $l_{\sigma,\mathrm{DEG}}/l_{\sigma,\mathrm{eth}}=1.2$ (see Table 1). The size data for various Al concentrations again show that particle concentration is not a significant factor controlling drop size.

Fig. 6 compares the drop-to-substrate impact velocities (u) for incipient drops of ethanol and DEG for voltage frequencies from 1 to 10 Hz. Impact velocities are estimated by measuring the distance traveled and the time interval between snapshots (using the Phantom 7.3, Vision Research high-speed camera) just before impact. The drop-impact velocities of both ethanol and DEG increase with frequency by a factor 60–75% for frequencies from 1 to 10 Hz. This is because the smaller drops (produced at higher frequency) are easier to accelerate from the nozzle under the assumed-constant electric field. Similar to the trend shown in Fig. 5, the impact velocity data for various Al concentrations also show that particle concentration is not a significant factor.

It is also notable in Fig. 6 that the impact velocity of the DEG-based ink is greater than that for the ethanol-based ink by 0.25–0.4 m/s and it is not clear why. It could be due to DEG's higher conductivity that is subject to greater electrostatic force.

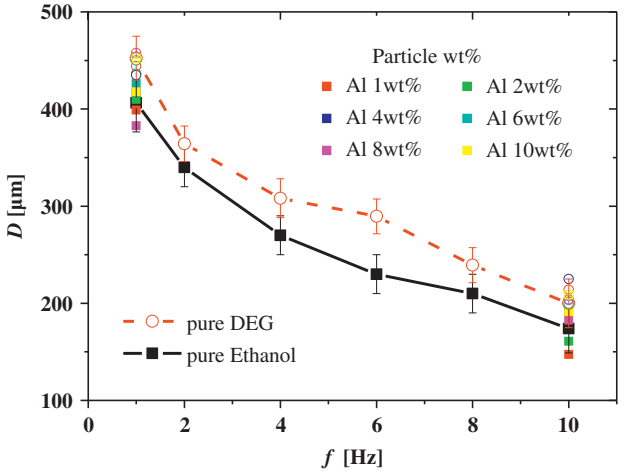

Fig. 5. Effect of Al wt% on the drop size for various voltage frequencies. The characteristic lengths (i.e., $l_{\mathrm{char}}=\mu^2/(\rho\sigma)$) of DEG and ethanol are $l_{\mathrm{char,DEG}}=29.6$ μm and $l_{\mathrm{char,eth}}=0.1$ μm, respectively.

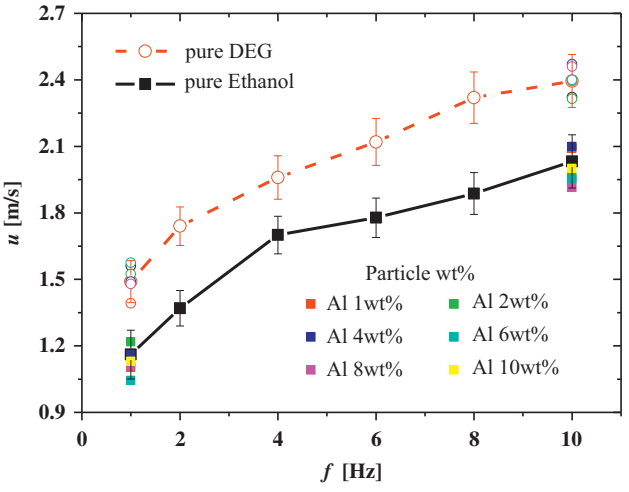

Fig. 6. Effect of Al wt% on the impact velocity for various voltage frequencies. The characteristic velocities (i.e., $v_{\mathrm{char}}=\sigma/\mu$) of DEG and ethanol are $u_{\mathrm{char,DEG}}=1.2$ m/s and $u_{\mathrm{char,eth}}=18.4$ m/s, respectively.

Fig. 7 shows the voltage required to ejected drops as a function of frequency. Unlike the previous experiments, Al particle concentration has a moderate effect on the required voltage when the working fluid's viscosity is low (e.g., ethanol). Increased Al concentrations necessitate a minor increase in charge. In an ideal conductor, charges reside at the fluid surface, but Al-based inks trap charge inside the fluid as Al concentrations increase, requiring additional voltage to destabilize the meniscus and generate a drop. On the other hand, when the ink's viscosity is high (e.g., DEG inks), the required voltage is not particularly sensitive to particle concentration or pulse frequency because the fluid properties (high μ) dominate. However, it should be noted that the applied voltage is the most sensitive variable in drop-generation stability and even modest changes to the voltage easily counter the effects of increased Al wt%.

Fig. 8 shows relics of the DEG-based ink containing 10 wt% Al; they are ~1 mm, comparable to the nozzle diameter. Although the ejected drop is one-half to one-third of the nozzle diameter, drop spread upon impact increases its size to 1 mm. Performance of the ethanol-based ink is similar to that of the DEG-based ink, except that the ethanol-based relics

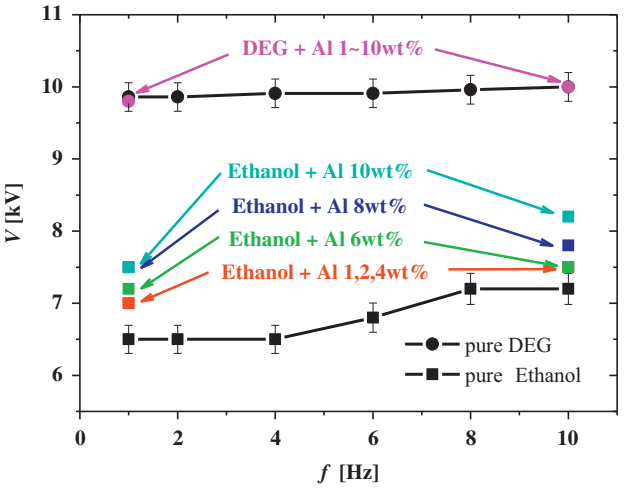

Fig. 7. Voltage required for stable drop formation at various voltage frequencies.

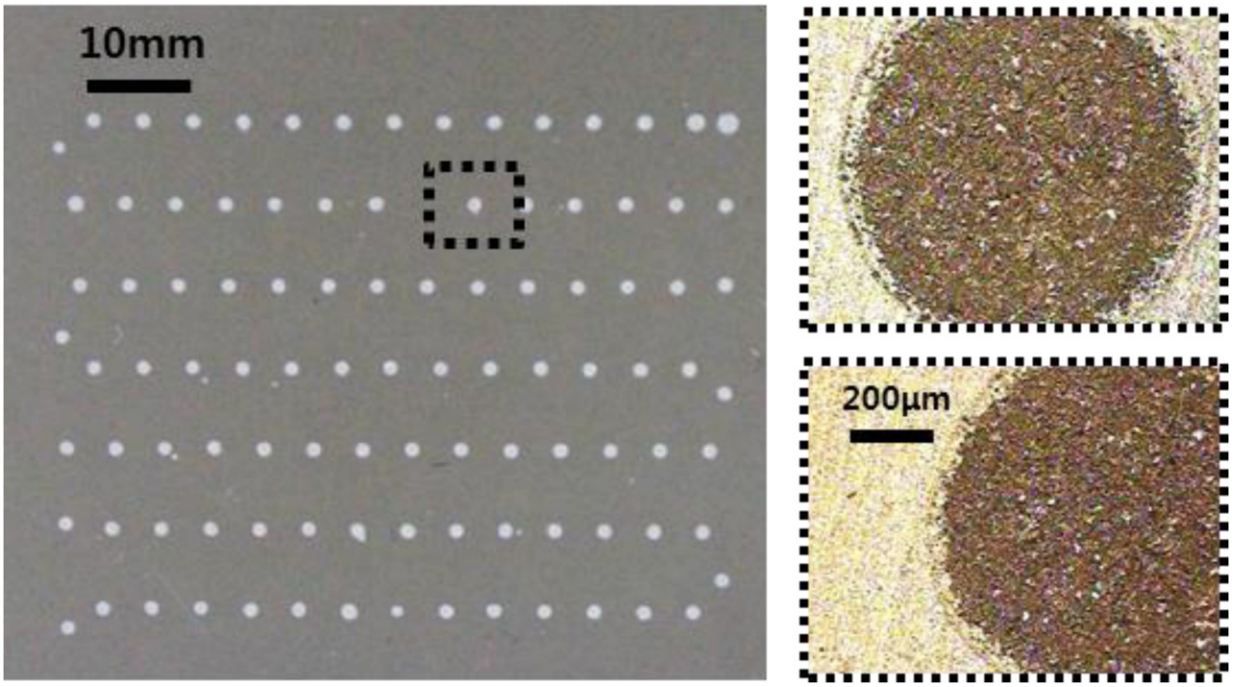

Fig. 8. Printed aluminum powder on a stainless-steel substrate (DEG ink, Al 10 wt%, f=1 Hz).

are a few times larger than those from DEG because ethanol's low viscosity allows increased spreading upon impact. Magnified views of the printed relics after complete evaporation of the solvent are shown in Fig. 8 (inset). An optical microscope was used to capture these snapshots. Although the Al particles are not optimally dispersed (some aggregation is observed), the relic maintains the desired circular shape. Because Al particles are of relatively large size, the coffee ring effect is not observed. This is another advantage of using large particles (i.e., non-nanoscale).

4. Conclusions

EHD inkjet printing technology had been explored for potential use in the printed electronics, especially for electrode manufacture. Ethanol, octanol, and DEG inks containing 1–10 wt% Al particles were studied. Ethanol-based-ink (low μ and σ) drop sizes are smaller than those from the DEG-based ink (high μ and σ). Also, the voltage required for drop generation depends on the fluid's μ and σ. The higher the μ and σ, the greater the required voltage. Drop sizes decreased and impact velocities increased when the voltage frequency increased. The distance required for complete drop separation from the nozzle decreased with increasing voltage frequency. The nozzle-to-drop separation distance was larger for DEG than for ethanol because DEG's has higher μ and σ. While the required voltage for DEG-based-ink drop generation was not affected by Al concentration, increased Al concentrations in the ethanol ink required slightly increased voltages for drop generation. For the range of 1–10 wt% considered in this study, particle concentration did not significantly affect the drop-generation characteristics. Rather, the ink's electro-fluid properties were the dominant factors that determined drop characteristics and printing quality.

Acknowledgment

This work was supported by the Center for Inorganic Photovoltaic Materials NRF-2011-0007182 and 2010-0010217 funded by the Korean government (MEST). This research was also supported by the Converging Research Center Program through the Ministry of Education Science and Technology (2010K000969). This work was also supported by the Human Resources Development of the Korea Institute of Energy Technology Evaluation and Planning (KETEP) grant funded by the Ministry of Knowledge Economy, Republic of Korea (No. 20104010100640).

References

Byun, D.Y., Lee, Y., Tran, S.B.Q., Nugyen, V.D., Kim, S. Park, B., et al. (2008). Electrospray on superhydrophobic nozzles treated with argon and oxygen plasma. *Applied Physics Letters*, *92*, 093507.

Chen, C.H., Saville, D.A., & Aksay, I.A. (2006). Electrohydrodynamic "drop-and-place" particle deployment. *Applied Physics Letters*, *88*, 154104.

Chen, P.H., Chen, W.C., & Chang, S.H. (1997). Bubble growth and ink ejection process of a thermal ink jet printhead. *International Journal of Mechanical Sciences*, *39*, 683–695.

Chen, P.H., Peng, H.Y., Liu, H.Y., Chang, S.L., Wu, T.I., & Cheng, C.H. (1999). Pressure response and droplet ejection of a piezoelectric inkjet printhead. *International Journal of Mechanical Sciences*, *41*, 235–248.

Cheng, K., Yang, M.H., Chiu, W.W., Huang, C.Y., Chang, J. Ying, T.F., et al. (2005). Ink-jet printing, self-assembled polyelectrolytes, and electroless plating: Low cost fabrication of circuits on a flexible substrate at room temperature. *Macromolecular Rapid Communications*, *26*, 247–264.

Choi, H.K., Park, J.-U., Park, O.O., Ferreira, P.M., Georgiadis, J.G., & Rogers, J.A. (2008). Scaling laws for jet pulsations associated with high-resolution electrohydrodynamic printing. *Applied Physics Letters*, *92*, 123109.

Duft, D., Achtzehn, T., Muller, R., Huber, B.A., & Leisner, T. (2003). Rayleigh jets from levitated microdroplets. *Nature*, *42*, 128.

Hughes, D.F.K., Robb, I.D., & Dowding, P.J. (1999). Stability of copper phthalocyanine dispersions in organicm media. *Langmuir*, *15*, 5227–5231.

Jaworek, A., & Sobczyk, A.T. (2008). Electrospraying route to nanotechnology: An overview. *Journal of Electrostatics*, *66*, 197–219.

Jayasinghe, S.N., Edirisinghe, M.J., & Wilde, T.D. (2002). A novel ceramic printing technique based on electrostatic atomization of a suspension. *Materials Research Innovations*, *6*, 92–95.

Kim, J.H., Oh, H.C., & Kim, S.S. (2008). Electrohydrodynamic drop-on-demand patterning in pulsed cone-jet mode at various frequencies. *Journal of Aerosol Science*, *39*, 819–825.

Korkut, S., Saville, D.A., & Aksay, I.A. (2008). Collodial cluster arrays by electrohydrodynamic printing. *Langmuir*, *24*, 12196–12201.

Lee, S.H., Byun, D.Y., Jung, D.W., Choi, J.Y., Kim, Y.J. Yang, J.H., et al. (2008). Pole-type ground electrode in nozzle for electrostatic field induced drop-on-demand inkjet head. *Sensors and Actuators A*, *141*, 506–514.

Marginean, I., Nemes, P., Parvin, L., & Vertes, A. (2006a). How much charge is there on a pulsating Taylor cone? *Applied Physics Letters*, *89*, 064104.

Marginean, I., Nemes, P., & Vertes, A. (2006b). Order-chaos-order transitions in electrosprays: The electrified dripping faucet. *Physical Review Letters 97*, 064502.

Miao, P., & Xiao, P. (2002). Formation of ceramic thin films using electrospray in cone-jet mode. *IEEE Transactions on Industry Applications*, *38*, 50–56.

Mishra, S., Barton, K.L., Alleyne, A.G., Ferreira, P.M., & Rogers, J.A. (2010). High-speed and drop-on-demand printing with a pulsed electrohydrodynamic jet. *Journal of Micromechanics and Microengineering*, *20*, 095026–095033.

Paine, M.D. (2009). Transient electrospray behaviour following high voltage switching. *Microfluid Nanofluid*, *6*, 775–783.

Paine, M.D., Alexander, M.S., Smith, K.L., Wang, M., & Stark, J.P.W. (2007). Controlled electrospray pulsation for deposition of femtoliter fluid droplets onto surfaces. *Journal of Aerosol Science*, *38*, 315–324.

Park, J.H., & Moon, J.H. (2006). Control of colloidal particle deposit patterns within picoliter droplets ejected by ink-jet printing. *Langmuir*, *22*, 3506–3513.

Park, J.U., Hardy, M., Kang, S.J., Barton, K., Adair, K. Mukhopadhyay, D.K., et al. (2007). High-resolution electrohydrodynamic jet printing. *Nature Materials*, *6*, 782–789.

Rayleigh, L. (1882). On the equilibrium of liquid conducting masses charged with electricity. *Philosophical Magazine*, *14*, 184–186.

Samarasinghe, S.R., Pastoriza-Santos, I., Edirisinghe, M.J., Reece, M.J., & Liz-Marzán, L.M. (2006). Printing gold nanoparticles with an electrohydrodynamic direct-write device. *Gold Bulletin*, *39*, 48–53.

Singh, M., Haverinen, H.M., Dhagat, P., & Jabbour, G.E. (2010). Inkjet printing—process and its applications. *Advancd Materials*, *22*, 673–685.

Stachewicz, U., Dijksman, J.F., Burdinski, D., Yurteri, C.U., & Marijnissen, J.C.M. (2009). Relaxation times in single event electrospraying controlled by nozzle front surface modification. *Langmuir*, *25*, 2540–2549.
Wasan, D.T., Nikolov, A.D., & Brenner, H. (2001). Droplets speeding on surfaces. *Science*, *291*, 605–606.
Xu, T., Jin, J., Gregory, C., Hickman, J.J., & Boland, T. (2005). Inkjet printing of viable mammalian cells. *Biomaterials*, *26*, 93–99.
Yarin, A.L., Koombhongse, S., & Reneker, D.H. (2001). Taylor cone and jetting from liquid droplets in electrospinning of nanofibers. *Journal of Applied Physics*, *90*, 4836–4846.